Reprinted from *Estuarine, Coastal and Shelf Science* (1995) **41**, 545–565

Modelling the Primary Production in the North Sea using a Coupled Three-dimensional Physical–Chemical–Biological Ocean Model

Morten D. Skogen, Einar Svendsen, Jarle Berntsen, Dag Aksnes and Kåre B. Ulvestad

Estuarine, Coastal and Shelf Science (1995) **41**, 545–565

Modelling the Primary Production in the North Sea using a Coupled Three-dimensional Physical–Chemical–Biological Ocean Model

Morten D. Skogen[a], Einar Svendsen[a], Jarle Berntsen[b], Dag Aksnes[c] and Kåre B. Ulvestad[c]

[a]Institute of Marine Research, Pb. 1870, Nordnes, N-5024, Bergen, Norway, [b]Department of Mathematics, University of Bergen, Norway and [c]Institute of Fishery and Marine Biology, University of Bergen, Norway

Received 30 September 1993 and in revised form 1 September 1994

Keywords: numerical model; phytoplankton; nutrients; primary production; transport; North Sea

A coupled three-dimensional physical–chemical–biological model system has been implemented, and applied to study mass and volume transports and primary production throughout the North Sea. The model was run twice for the year 1985 with specified (for the North Sea Task Force) time series of riverine and atmospheric inputs of nutrients, and also with these nutrient inputs reduced by 40 and 50%, respectively. In particular, the evolution of the chemical and biological variables in the two situations was studied. The model output agreed quite well with the general quantitative and qualitative knowledge of the total yearly production. The intercomparison with some salinity profiles also indicated that the model handles the large-scale circulation and vertical mixing fairly well. Estimates for the transport of excess nutrients to Skagerrak and Kattegat in the highly pulsating Jutland coastal current are given. The estimates demonstrate the need for such models for calculating transport of matter from one area to another. Significant reductions in both primary production and transport of matter were seen from comparisons between the two runs.

Introduction

There is an increasing concern about the ecological effects of increased anthropogenic nutrient inputs to the ocean. The primary production is affected by the changes in nutrient inputs, and in many areas this has caused severe problems. There seems, for example, to have been an increasing trend of harmful flagellate blooms in the coastal areas of the southern North Sea. Probably the most extreme case was the *Chrysocromolina polylepis* bloom in the spring of 1988 extending as far north as the Norwegian west coast (Dundas *et al.*, 1989; Maestrini & Graneli, 1991).

It is also important to quantify and study the variability in space and time of the primary production because of its importance as a possible regulating mechanism for the fish production. However, measuring *in situ* primary production is a time

0272–7714/95/050545+21 $12.00/0

consuming and expensive task, and therefore relatively few measurements are available in either space or time. With the well-known patchiness of algae, rapid variability and uncertain amounts of recirculation of nutrients, gross estimates (from sparse data) of average production over a certain ocean area and over a certain time have very large uncertainties.

Related to the problems with algae, there has been an increasing political demand to the scientific community for answering the question: what will be the effects if the anthropogenic nutrient inputs to the North Sea are reduced, say, by 50%? Answers to such a question require the help of more or less sophisticated models depending of the sophistication of the answer and the hydrodynamics of the area of interest. Similarly, this is true for the question related to the food production being more related to the natural production variability.

A coupled physical–chemical–biological (P-C-B) modelling activity of the whole North Sea started in 1990–91 through close cooperation between the Institute of Marine Research (IMR) in Bergen, the Institute of Fishery and Marine Biology (IFM) at the University of Bergen, and the Norwegian Meteorological Institute (DNMI) in Oslo. Related to the above problem areas and that the North Sea as a whole is a fairly complex hydrodynamical system, it was found that to obtain any realism in the biological results, the coupled model system should be based on a sophisticated three-dimensional physical model that is able to represent the vertical exchanges realistically. Therefore, the physical module is based on a model by Blumberg and Mellor (1987). This model performed favourably in a recent Norwegian model-evaluating project (Martinsen *et al.*, 1990; Slørdal *et al.*, 1991), and it has been applied successfully to study circulation of many limited and diverse ocean areas such as Chesapeake Bay (Blumberg, 1977), the South Atlantic Bight (Blumberg & Mellor, 1983) and many others.

This coupled NORWegian ECOlogical Model system (NORWECOM: Skogen, 1993) is the basis for this paper focusing on modelling during 1985, and it has also been used (Aksnes *et al.*, 1995) for the simulation of the *C. polylepis* bloom. To keep the model system general, the parameterization of the chemical–biological interactions is based on information from available literature, and fine-tuning/calibration has been avoided.

After a description of the hydrodynamics and the chemical–biological modules, including initialization and limitations, we focus on the model results of spatial distribution and time evolution of primary production, the nutrients, diatom and flagellate concentrations in a few ICES boxes (Anon., 1983), the mass and volume transports through these boxes and through a section, vertical distribution at several points, and finally we discuss the modelled reduced production if the anthropogenic inputs of the nutrients are reduced by 50%.

The model

The model is implemented on an extended North Sea (see Figure 1), discretized in a 20×20 km grid. Vertically σ-coordinates with 11 layers are used following the bottom topography and chosen to give high resolution near the surface. At 100 m bottom depth, the layers are 0·5, 0·7, 1·3, 2·5, 5, 10, 20, 20, 20, 15 and 5 m thick (and 10 times this at 1000 m depth).

The model has a free surface and a split time step. The external mode portion of the model is two-dimensional and uses a short time step based on the CFL

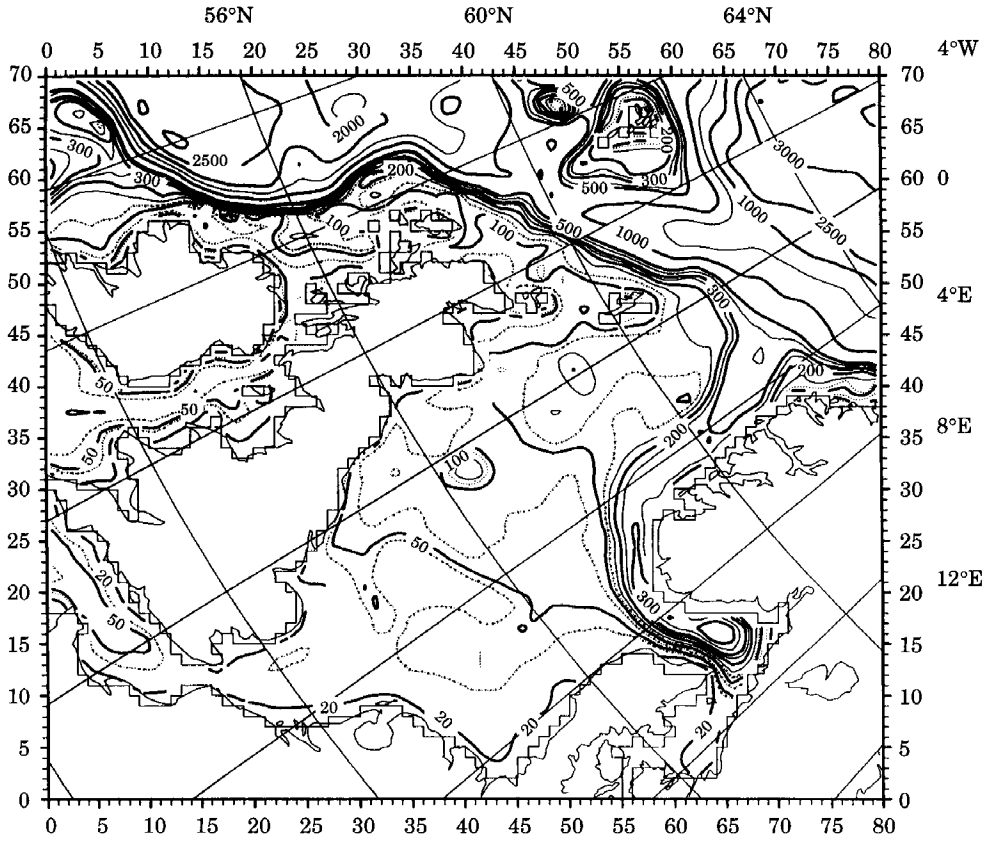

Figure 1. Model area, main bottom topography (in m) and horizontal resolution (20 × 20 km) indicated by zig-zag land contours. The outer seven grid cells of the open boundaries in the north, west and southwest belong to the FRS zone and are not realistically modelled.

(Courant Friedrichs Levy) requirement related to the *external* wave speed, while the internal mode is three-dimensional and uses a long time step based on the CFL condition related to the *internal* wave speed. In general, the model calculates all the P-C-B prognostic variables (see below) every internal time step, i.e. every 15 min. For the depth-integrated velocity an external time step of 30 s is used. Figure 2 demonstrates the concepts of the main processes and variables involved in the total model system.

Around the open boundaries a seven-gridcell ' flow relaxation scheme ' (FRS) zone is used (Martinsen & Engedahl, 1987). Each prognostic variable, φ, in the zone is simply updated by the translation $\varphi=(1-\beta)\varphi_{\text{int}}+\beta\,\varphi_{\text{ext}}$, where φ_{int} contains the time-integrated, unrelaxed values calculated in the entire model domain, i.e. also in the areas covered by the FRS zone, and φ_{ext} is the specified external solution in the zone. φ is the new value and β a relaxation parameter which varies from 0 at the end of the zone facing the interior model domain to 1 at the outer end of the zone. This simple FRS zone technique effectively absorbs inconsistencies between forced boundary conditions and model results.

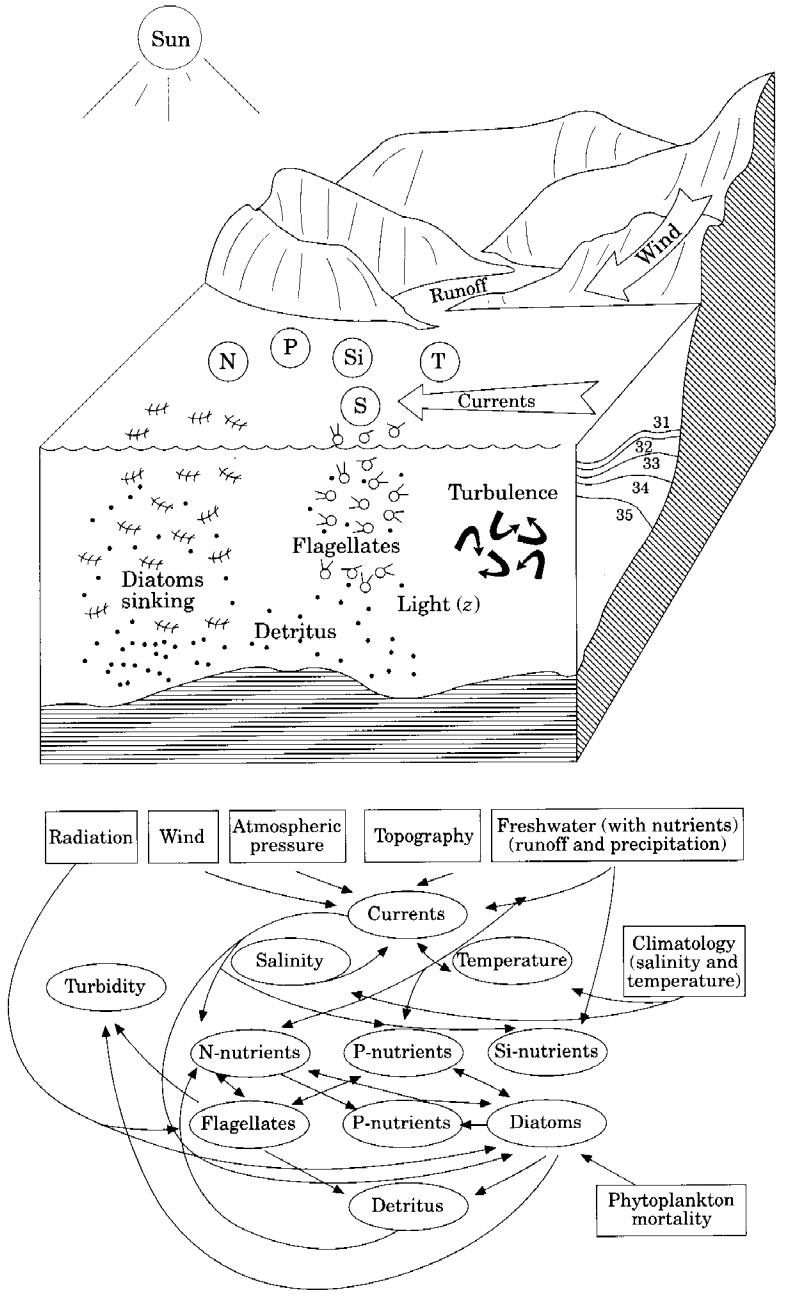

Figure 2. Schematics and diagram of the main coupled P-C-B processes involved in the model system.

Hydrodynamics

The approximation of the circulation in the North Sea is based on the three-dimensional (3-D), primitive equation, time-dependent, wind and density driven Princeton ocean model (POM) (Blumberg & Mellor, 1987; Mellor, 1993). The prognostic variables of this model are: (1) three components of the velocity field, (2) temperature, (3) salinity, (4) turbulent kinetic energy, (5) turbulent macroscale, and (6) water level.

The governing equations of the model are the horizontal momentum equations, the hydrostatic approximation, the continuity equation, conservation equations for temperature and salinity and a turbulence closure model for calculating the two turbulence variables (Mellor & Yamada, 1982). The equations and boundary conditions are approximated by finite difference techniques in an Arakawa C-grid (Mesinger & Arakawa, 1976).

The forcing variables are 6-hourly hindcast atmospheric pressure fields provided by DNMI (Eide *et al.*, 1985), 6-hourly wind stress (translated from the pressure fields by assuming neutral air–sea stability), four tidal constituents (M_2, S_2, K_1 and O_1) at open boundaries and freshwater runoff. Freshwater is added at each internal time step by increasing the water level at the cell closest to the river outlet according to the volume of freshwater discharged during the internal time step. The freshwater is mixed with the saline water down to 5 m. Monthly mean data from 12 European rivers are taken from Anon. (1992). In addition, extra freshwater is added at eight points along the Norwegian coast to equal estimated total freshwater runoff values from this coastline (Egenberg, 1993), which is believed to be a necessary condition for proper modelling of the Norwegian coastal current. The in/out-flow from the Baltic is calculated (Stigebrandt, 1980) from the modelled water elevation in the Kattegat and the climatological monthly mean freshwater runoff. This water entering Kattegat from the Baltic has a salinity near 8 all through the year. Since the temperature and salinity are prognostic variables, the density can also be defined as an implicit forcing variable.

In the lack of data on the surface heat fluxes, a 'relaxation towards climatology' method is used (Cox & Bryan, 1984). It is used such that during calm wind conditions, the surface temperature field would adjust to the climatological values after about 10 days (Oey & Chen, 1991). Climatological data for sea surface temperature are taken from (Martinsen *et al.*, 1992). The net evaporation precipitation flux was set to zero, except for an input of nitrate (see below).

The model is strongly dependent on two physical constants. One is a minimum value for the vertical eddy viscosity/diffusion coefficient, which is set equal to 2×10^{-5} m^2 s^{-1}, related to the velocity gradients, and 10^{-7} for the temperature and salinity gradients. The other is a dimensionless horizontal diffusion constant (here set to 0·2) used in connection with Smagorinsky's technique (Smagorinsky, 1963) for eliminating small scale ($2\Delta x$) velocity and density structures being produced in the model (and in nature), but not being resolved.

Chemical–biological dynamics

The prognostic variables are: (1) inorganic nitrogen (such as nitrate and ammonia), (2) inorganic phosphorus (phosphate), (3) inorganic silicon (silicate), (4) detritus (dead organic matter), (5) diatoms, (6) flagellates, and (7) light, turbidity.

The biological model is fully described in Aksnes *et al.* (1995) (see also Aksnes & Lie, 1990; Skogen, 1993). For completeness a short review of the main processes,

schematically shown in Figure 2, are given in Appendix A. A list of the values for the parameters in use are given in Appendix B.

The biological model is coupled to the physical model through the subsurface light, the hydrography and the horizontal and the vertical movement of the water masses. Phytoplankton production is affected by nutrients, surface irradiance, temperature and the attenuation/turbidity of the water. For both the dead and the living algae, sinking rates are applied also. Nutrients are added to the system from the many rivers and from the atmosphere (only nitrate). These data (nutrients and light) are all taken from Anon. (1992). Nutrient concentrations of the Baltic outflow are smoothed values from data provided by the International Council for the Exploration of the Seas (ICES) from a regular monitoring station located just inside the Belts (between Denmark and southern Sweden). Besides rivers and atmosphere, nitrogen and phosphate are regenerated from the dead algae, detritus, at a constant rate.

Initialization

The initial values for velocities, water elevation, temperature and salinity are taken from monthly climatologies for December (Martinsen *et al.*, 1992). Interpolation between monthly fields are also used at all the open boundaries, except at the inflow from the Baltic where the volume fluxes have been estimated from the modelled sea-surface elevation in Kattegat (Stigebrandt, 1980) and the climatological mean freshwater runoff.

For simulating 1985, nutrient fields are derived and extrapolated/interpolated (Ottersen, 1991) from February 1988 data (obtained from ICES and taken to represent 15 December 1984), together with some small initial amounts of diatoms and flagellates (2·75 mg N m^{-3}). Very few (continuous) time series of nutrients are available from the inflow of Atlantic water. At the open boundaries (outside the North Sea) nutrient values from station M (66°N,2°E) from 1992 (Rey, pers. comm.,) have been used and assumed valid everywhere in the inflow area. Nutrient data (monthly means) measured in the Baltic (ICES) are used for the water flowing into Kattegat.

Limitations

The model does not at present incorporate ' real ' surface heat fluxes, surface irradiance and surface freshwater fluxes (direct rain and evaporation). There are no zooplankton eating the algae, and no ' particle ' bottom settlement and resuspension routines are incorporated in the model. Neither are there, at present, routines for regeneration of silicate, which means that the model can be run, at most, one year at a time. Processes such as material bindings to dissolved organic material (DOM), colloides and particles of different sizes (and flocculation) also affect the sedimentation and resuspension rates, but are not included. Clearly, the horizontal grid resolution is a limiting factor with respect to correct simulation of, for example, near-shore and mesoscale processes. A very clear limitation is the lack of realistic light attenuation due to riverine inputs of gelbstoff, suspended particulate matter and resuspended sediments.

Primary production results

The model enables output of all P-C-B prognostic variables in all points at every internal time step (15 min). Nevertheless, this paper mostly concentrates on the chemical–biological results it provides.

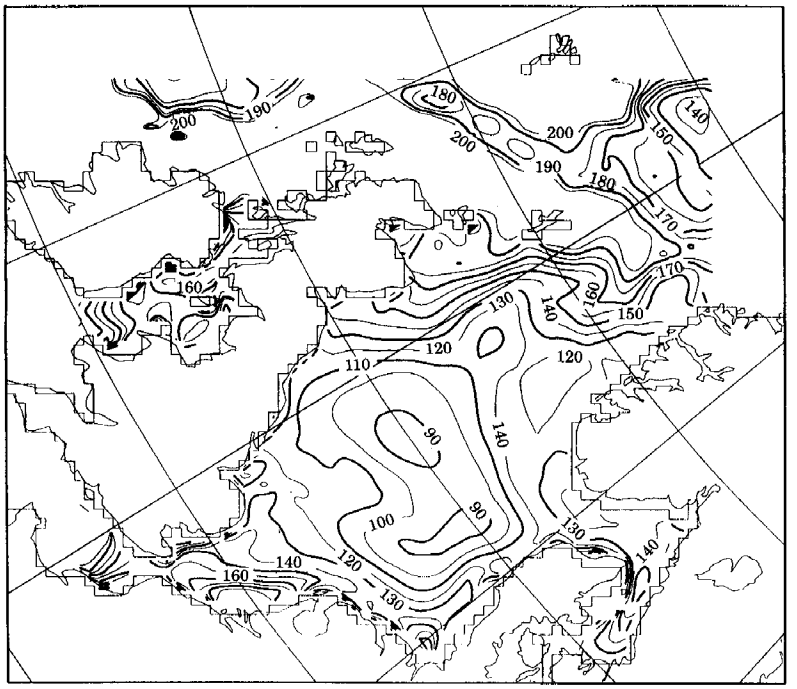

Figure 3. Modelled annual depth-integrated production (g C m^{-2} $year^{-1}$).

Figure 3 shows the total depth-integrated annual production per m^2 of surface, for the whole model domain. (Note that in this and all of the following horizontal plots results from the FRS zone, which is not properly modelled, are omitted.)

The results compare quite well with what are thought to be realistic numbers for the productivity (see e.g. Holligan, 1989; Joint & Pomroy, 1992), with a total production of almost 90 g C m^{-2} $year^{-1}$ in the central North Sea and more than 200 g C m^{-2} $year^{-1}$ in coastal waters in the south. In the northern parts, the production may seem somewhat high. The main reason for this is probably a combination of vertical resolution, steep topography and the sigma-coordinate system causing high mixing of the nutrient-rich Atlantic water, but very little is known about the annual production in these deep-water areas.

Comparing the model results with estimates given in the North Sea Quality Status Reports (QSR) 1993, with respect to ICES boxes (see Figure 4), the results are also quite promising. In Table 1 results from NORWECOM (mean production in each box together with the interval in which the production varies within each box) are compared to results from Joint & Pomroy (1992) and a few QSRs (Anon., 1993*a,b,c,d,e*).

In Figure 5, total production (Figure 3) has been separated into a diatom and a flagellate part. The diatom part of the production increases from south to north where silicate from the Atlantic water is pumped into the model domain. This is the main reason for the large total production in these areas. Clearly, since diatoms have a higher light affinity they can produce at much weaker light conditions than the flagellates. The silicate limitation in most of the North Sea is a very strong regulator for the balance between diatoms and flagellates.

TABLE 1. Primary production (g C m^{-2} $year^{-1}$) comparison between model results (mean and interval), estimates from the NERC North Sea project (August 1988–October 1989) and QSRs from 1993

Subarea	NERC	QSR-93	NORWECOM	NORWECOM
1		150	157	110–200^{+}
3a	75		148	100–200
3b	79		124	100–160
4	199	(100–400)	152	110–200^{+}
5	261		125	100–200^{+}
6		100–130	126	110–170
7a	100	100	101	90–130
7b	119		104	90–130

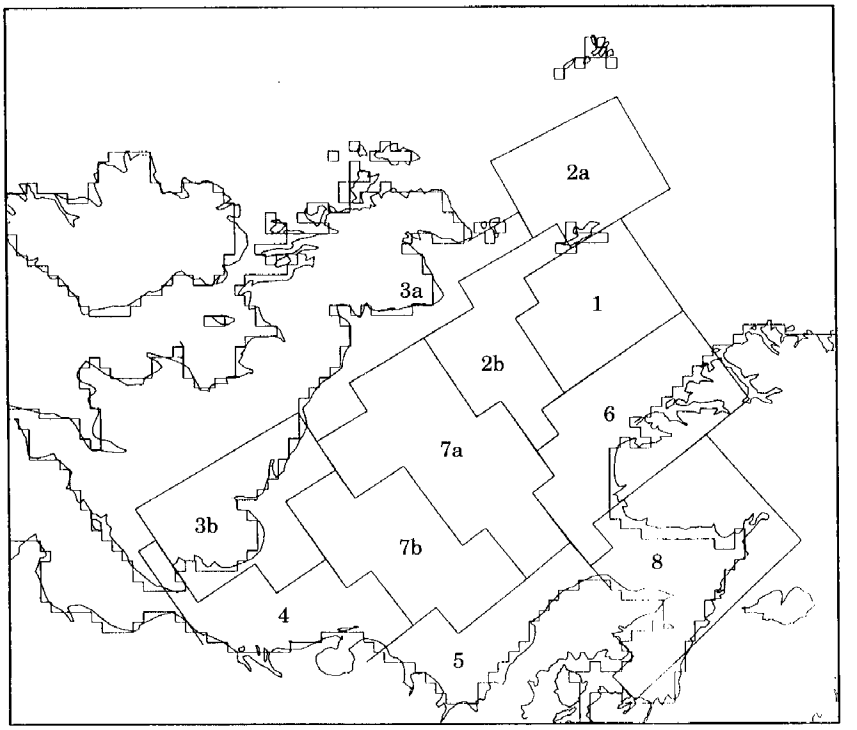

Figure 4. ICES subareas.

Production is known to have strong seasonal variations with a diatom bloom in February–April (which depends on the latitude in the sense of moving northwards in time), followed by a bloom of flagellates which ends in July–August. It starts in the nutrient-rich areas just outside the largest continental river mouths and spreads north as the daily irradiance (and temperature) increases with season. Owing to high turbidity and heavy nutrient input, the near-shore coastal zone typically has a surplus of nutrients and the growth of phytoplankton is limited by light. The extent of this is largest in winter when the amount of incoming light is low and the discharge of freshwater and nutrients is high. Silicate is typically the first nutrient to become limiting in spring, causing the termination of spring diatom bloom in the coastal waters (Gieskes & Kraay, 1975). The

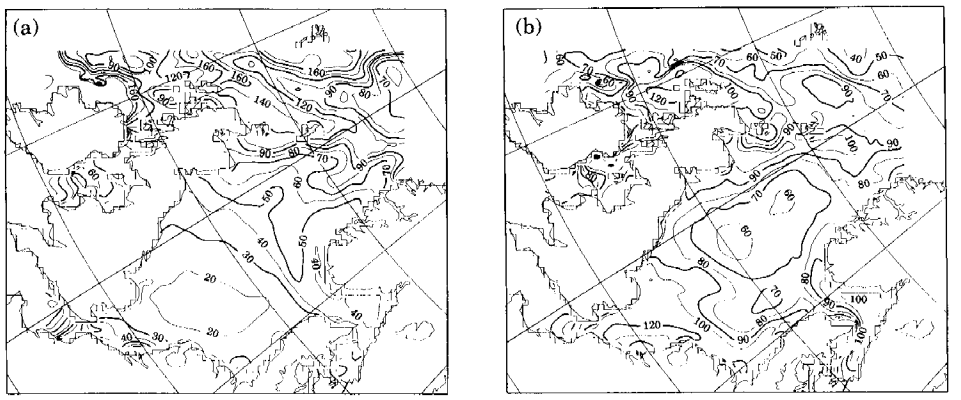

Figure 5. Modelled annual depth-integrated production (g C m^{-2} $year^{-1}$) of (a) diatoms and (b) flagellates.

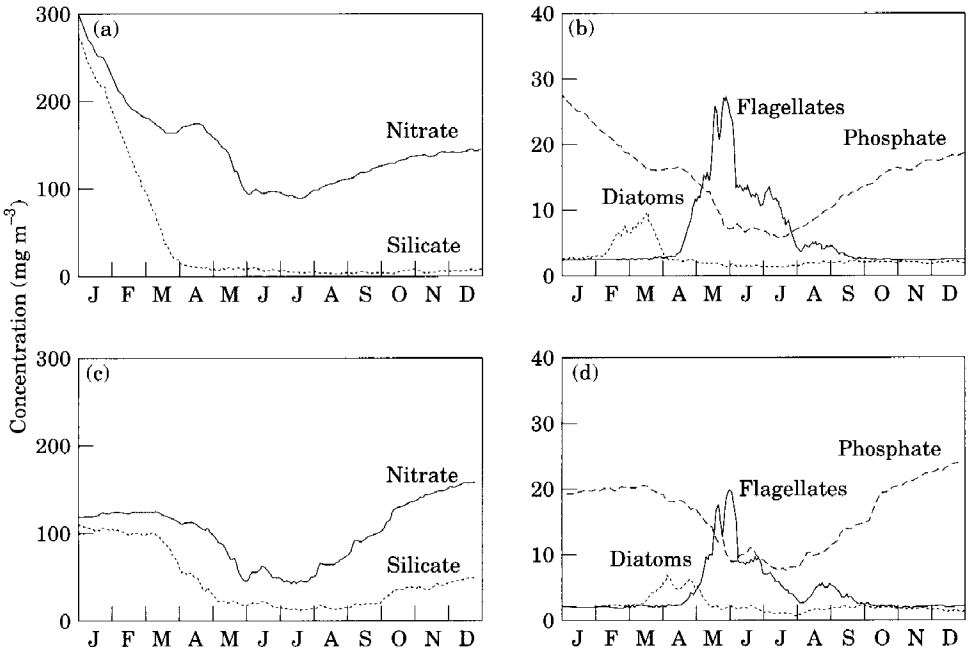

Figure 6. (a,c) Nitrate and silicate, together with (b,d) flagellates, diatoms and phosphate in the upper 30 m of (a,b) ICES box 5 and (c,d) ICES box 6.

remaining nitrogen and phosphorus allow further growth of algae not requiring silicate. Reflecting the high N/P ratio of the riverine nutrient input, phosphorus is typically the second nutrient to become limiting in coastal waters. This has clearly been demonstrated in data from the late 1980s (Lancelot *et al.*, 1989).

These seasonal variations have been investigated. In Figure 6, time series of daily mean modelled 3-D average concentrations of nitrate and silicate together with the same numbers for phosphate, diatoms and flagellates in the upper 30 m of ICES boxes 5 (German bight and west of Denmark as far north as Hanstholm)and 6 (further north along the Norwegian west coast to Sognefjorden) through the modelled year are given.

The diatom bloom deteriorates as all available silicate is used in the production. Also, for the flagellate bloom, a strong correlation between the plankton concentration and the available nutrients can be seen. Keeping in mind that the production is set to use nitrogen and phosphorus according to the Redfield ratio (N/P=16 atomic, corresponding to 7·24 weight/weight), see Appendix B, it is clearly seen that the lack of phosphate is the main reason for limiting the production of flagellates in area 5 with its high amount of excess nitrate. In subarea 6, with a lower level of eutrophication and high influence of Atlantic water, no lack of phosphate is seen; however, there is a tendency to lack nitrate. For the averaged values in the upper 30 m there is no serious imbalance, but looking at the upper 20 m the nitrate limitation is clearly seen.

The developing blooms can be followed from south to north in time. In the southernmost box 5 the diatom concentration reaches its maximum in February–March, and the flagellate blooms starts mid-April with a maximum in May, while in the northern box 6, the diatom maximum is mid-April with a flagellate bloom starting in May.

Compared with the phytoplankton stations sampled monthly from January to May 1989 in ICES box 5 (Anon., 1993*c*), the new phytoplankton stocks developed up to March, and in May a rapid growth of phytoplankton was observed, which in seasonal sense agrees quite well with what the model shows.

The model simulation of this box (no. 5) gives a mean summer concentration of nitrate which is a little lower than 100 mg m^{-3} (7 μM) and agrees quite well with the mean summer concentrations from 1985 (8 μM) given in the same report. The corresponding numbers for phosphate are 7 mg m^{-3} (0·23 μM) and 0·6 μM. The values from winter 1984–85 (initialization) also agrees quite well. At the end of the model period both nitrate and phosphate seems too low compared with typical winter values. These values will vary from year to year, but the inclusion of sedimentation/resuspension processes seems crucial if the model is to be run more than one annual cycle.

In subarea 6, where sedimentation/resuspension is less important for the available nutrients in the upper 30 m, we observed that both nitrate and phosphate returns to their initial states after 1 year of simulation. Also, 150 mg m^{-3} (10·7 μM) of nitrate and 23 mg m^{-3} (0·75 μM) of phosphate agree quite well with what are believed to be typical winter values in this area (Anon., 1993*d*).

A better view of the developing production can be obtained by studying the horizontal distribution of the production (g C m^{-2} $month^{-1}$). In Figure 7, the flagellate production in April, May, June and August is given. The model clearly produces a bloom starting outside the southern coastal areas which moves north with season, and deteriorates as the nutrients diminish.

Hydrography and transport of water masses

At selected points all prognostic variables were stored as daily means in all σ-depths. Two of these points were chosen; one (57°44′N, 6°30′E) close to Lista at the southern tip of Norway, and one in the German bight (54°17′N, 7°35′E).

Close to the Lista point (58°01′N, 6°32′E) the Institute of Marine Research regularly monitors the salinity. In Figure 8, time series for salinity, both modelled and measured, at Lista are given. The model seems to reproduce many of the main characteristics. It keeps the salinity gradient close to the surface, responds to up- and downwelling, keeps the salinity 34·5 isoline between 50 and 100 m depth and shows the characteristic

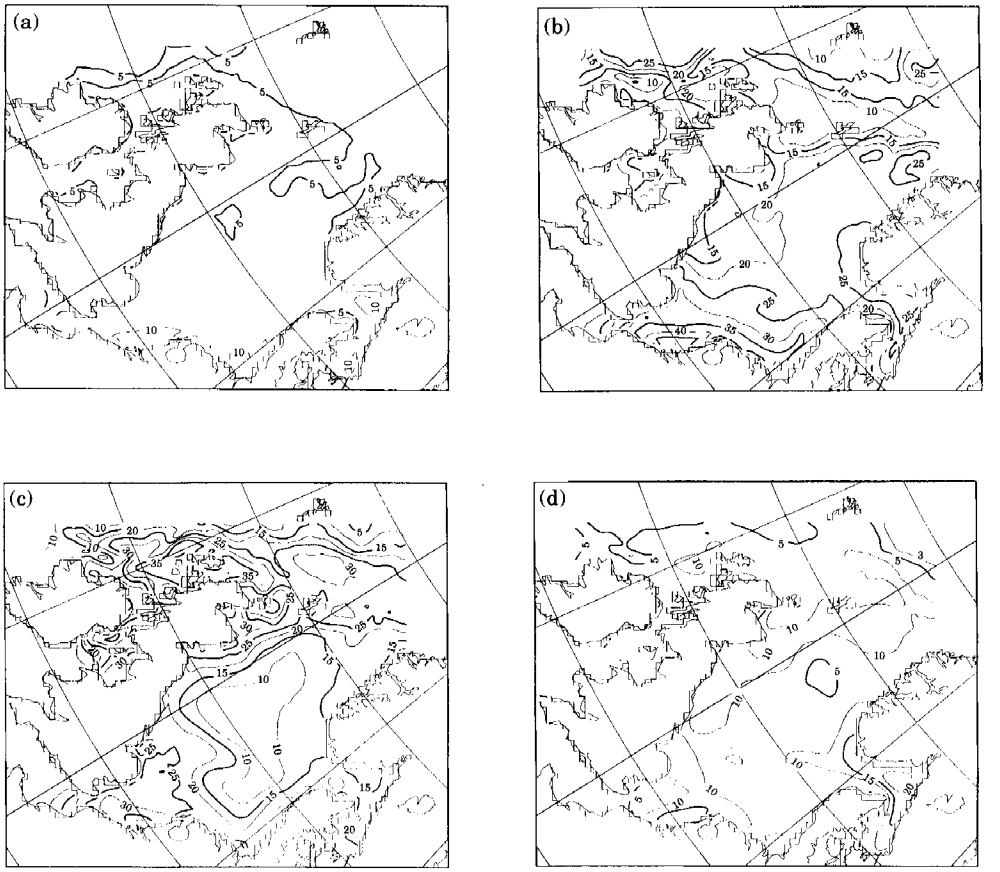

Figure 7. Production of flagellates (g C m^{-2} $month^{-1}$) in (a) April, (b) May (c) June and (d) August.

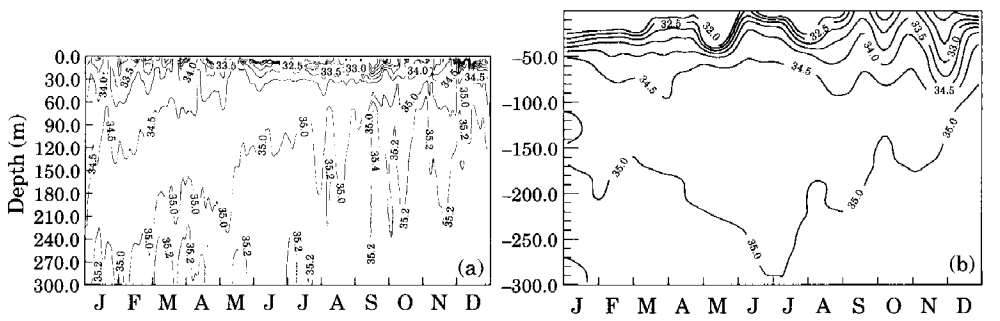

Figure 8. (a) Modelled and (b) measured salinity at Lista.

situation where saline water moves towards the surface during autumn 1985. The similarities between modelled and measured salinity are a good indicator for the vertical mixing/entrainment of nutrients being realistically modelled, crucial for realistic estimates of primary production.

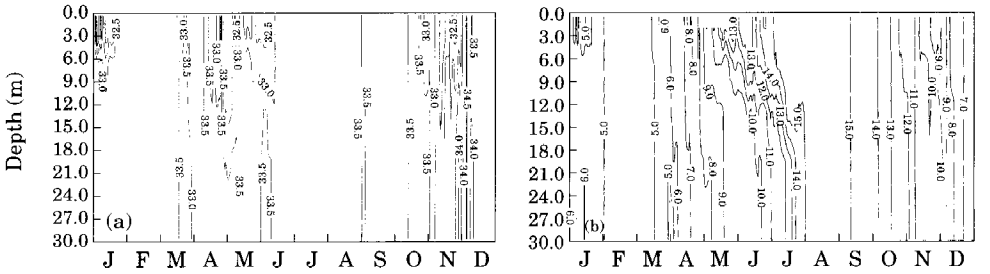

Figure 9. Modelled (a) salinity and (b) temperature at the German Bight point.

The German Bight water (Figure 9) is well mixed with a salinity of about 33·5, and is seasonally stratified in the period April–June, when the temperature increases from 7 to 14 °C. The stratification in November and January also coincides with thermal stratification.

Compared to climatological fields (Damm, 1989) the modelled water seems to be too well mixed since the climatology gives a less saline upper layer most of the year, but the salinity of the bottom water (33·5) agrees quite well with climatological data in the salinity interval 33·0–33·5. For the temperature the results seem to be very promising. Except for too high minimum and too low maximum values, the rest of the year is within 1 °C of the climatological temperatures (Damm, 1989).

Since NORWECOM generates its own 3-D current pattern, it enables the modelling of realistic variations in the flow structure and transport, with the chemistry and biology in dynamic balance. It is therefore assumed that by keeping the high time resolution resolving the short-time variability, any long-term average will be much more realistic.

Let u be the instantaneous velocity. It can be separated into a mean (in time) velocity $\bar{u}$ and a fluctuating part, $\dot{u}$, such that $u=\bar{u}+\dot{u}$. The cross-boundary advective import of matter, has been defined as:

$$\bar{F}_{\mathrm{adv}}=\int_A \bar{c}\ \bar{u}_{\mathrm{in}}$$

where A is either a section or part of the boundary of a box, $\bar{c}$ is a mean concentration, and $\bar{u}_{\mathrm{in}}$ is a mean velocity (normal to dA) in each gridcell of A. This means that dispersive exchange caused by variabilities shorter than the averaging period has been omitted.

In Figure 10, the modelled mean annual cross-boundary advective inflow, residence time and annual cross boundary advective transport of total (i.e. organic and inorganic) nitrogen into the ICES subareas (see Figure 4) are given. Note that the residence time is here defined as the ratio between box volume and flow, and that the annual flow in subarea 6 is 440.

The residence time (and thereby flow) agrees quite well with some other model estimates from subarea 4, 7b and 1 (de Vries, 1992).

The transport through most of the subarea is larger than the generally accepted value (causing shorter residence times). There might be several reasons for this. The modelled currents may in general be too strong, or there may be more or less stationary mesoscale circulation that crosses the boundaries at several places, thereby causing the same flow to be added several times. This is especially the case for subarea 6 (see Figure 4) along the Norwegian west coast, where the main flow is parallel to the longest box wall. The

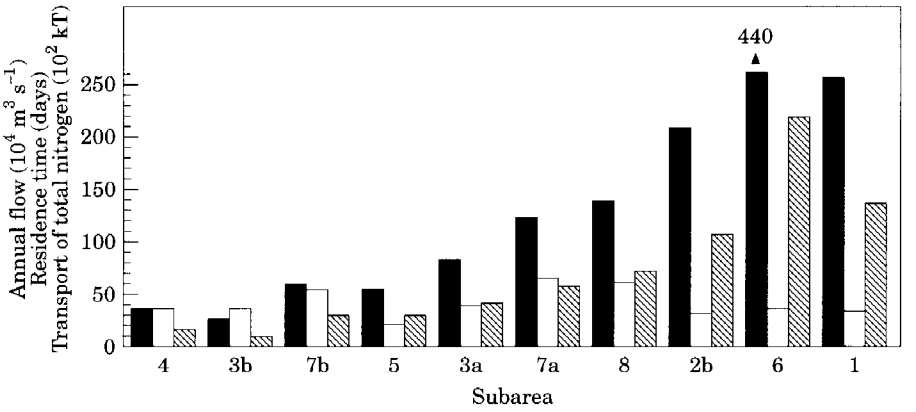

Figure 10. Modelled mean annual cross-boundary advective inflow (■), residence time (□) and annual cross-boundary advective transport of total nitrogen (▨) to the ICES subareas.

estimation of this transport leaves a problem in the sense of choosing a proper length scale in the averaging of u, in the sense of avoiding mesoscale eddies and meanders. With 20-km horizontal resolution many of these features are included, but to extend the averaging to more than one gridcell might eliminate the general circulation pattern in some areas. In addition to this, some of the subareas are defined without paying enough attention to the general circulation, leaving problems, such as flow parallel to the box walls.

An important issue, especially concerning primary production and sedimentation of pollutants in the Skagerrak/Kattegat area, is the transport of nutrient-rich water from the southern North Sea and the German Bight into this region. Much effort has been put into the work of identifying and quantifying the different water masses entering and leaving the Skagerrak area and their variation over time. It has also been important to investigate the mechanisms that drive the circulation and to study their effect on biological processes (Danielsen *et al.*, 1992). Defining water entering Skagerrak from the German Bight as water with salinity between 31 and 34 and inorganic nitrogen higher than 1 μM the mean (25 h) net advective transport of inorganic nitrogen from the German Bight through a part of the SKAGEX section H (from 56°38′N, 8°10′E) at the Danish west coast close to the Limfjorden outlet (to 57°12′N, 7°23′E), at 50 m depth, has been estimated. The results (in − out) excluding the dispersive exchange due to tides, are given in Figure 11. Note that the estimate does not exclude the mean advection caused by the tide, it only excludes the tidal dispersion being directly coupled to the cross-sectional gradient of the nitrogen concentration. Previous estimates suggest that the dispersion in this area is about 2% of the advective transport.

It is interesting to note these strong inflows in short pulses. Since this behaviour is difficult to measure without continuous monitoring, realistic transports and flows can only be obtained through such modelling efforts.

The total net advective transport of nitrate with the Jutland current from the German Bight and into Skagerrak during 1985 is calculated to be 250 kT (kilo tons), from the model with an average flow of 0·07 Sverdrup. This agrees quite well with some other estimates of the same transport of about 400 kT and 0·15 Sverdrup (Skjoldal, 1993). However, this result disagrees with measurements by Rydberg (1993) suggesting this

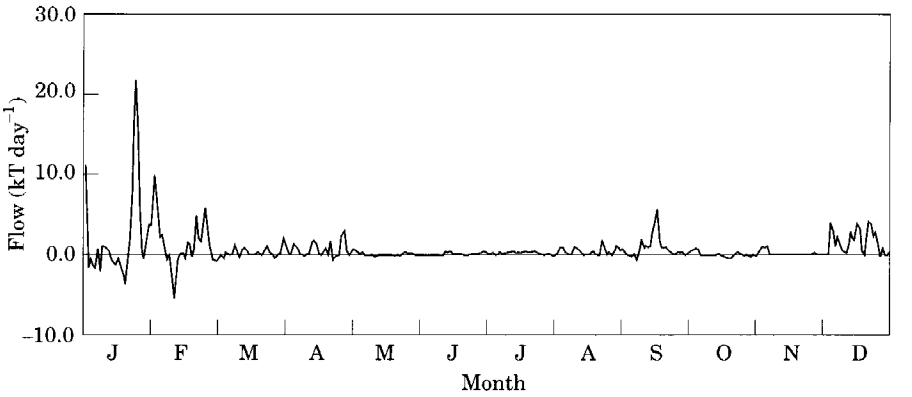

Figure 11. Net advective transport of nitrate through section H. Salinity between 31 and 34. Nitrate >1·0 μM.

flow to be negligible. With the variability shown in Figure 11, and knowing that Rydberg's measurements were never performed in rough weather, we postulate that a representative mean is not obtained by his method.

An application to eutrophication

Many projects are devoted to the question on the effect of anthropogenic deposition to the primary production (see e.g. de Vries, 1992). The interest in this issue has increased together with the many blooms of toxic algae in recent years (Aksnes *et al.*, 1989; Dundas *et al.*, 1989; Skjoldal & Dundas, 1989). At the '2nd International Conference on the Protection of the North Sea' (London 1987), all countries around the North Sea agreed on reducing the input of nutrients by 50% between 1985 and 1995 in those areas where nutrients cause, or are likely to cause pollution. An additional run of the model with a 40% reduction (80% of the total load is assumed anthropogenic) of the loads of inorganic nitrogen and phosphorus from rivers (included deposition from the Baltic Sea) and 50% reduction of the input of inorganic nitrogen from the atmosphere was made. The production fields were then compared to try to get a picture of what effects this would have during the first year, assuming an immediate reduction. Note that the initial field and the inflow in the FRS zone are identical in both runs.

Since there is no reduction in the input of silicate, which is rate-limiting for the diatoms, the influence on their production is negligible. The main effect caused by this reduction will therefore be on the production of flagellates. In Figure 12, the reduction (given as percentage) of the depth-integrated annual production (g C m^{-2}) and the production per month for April, June and August for flagellates are given. The local effects are significant, with a reduction of more than 25% close to the southern estuaries on a monthly basis (15–20% annual). The overall reduction (annual) in large areas of the North Sea are in the interval 5–10%. With a horizontal resolution of 20 km and a minimum depth of 10 m the coastline is not properly resolved. In addition, numerical diffusion smooths out the fields, so locally the reduction in many coastal areas is believed to be bigger. On the other hand, in these areas the offshore reduction might be overestimated.

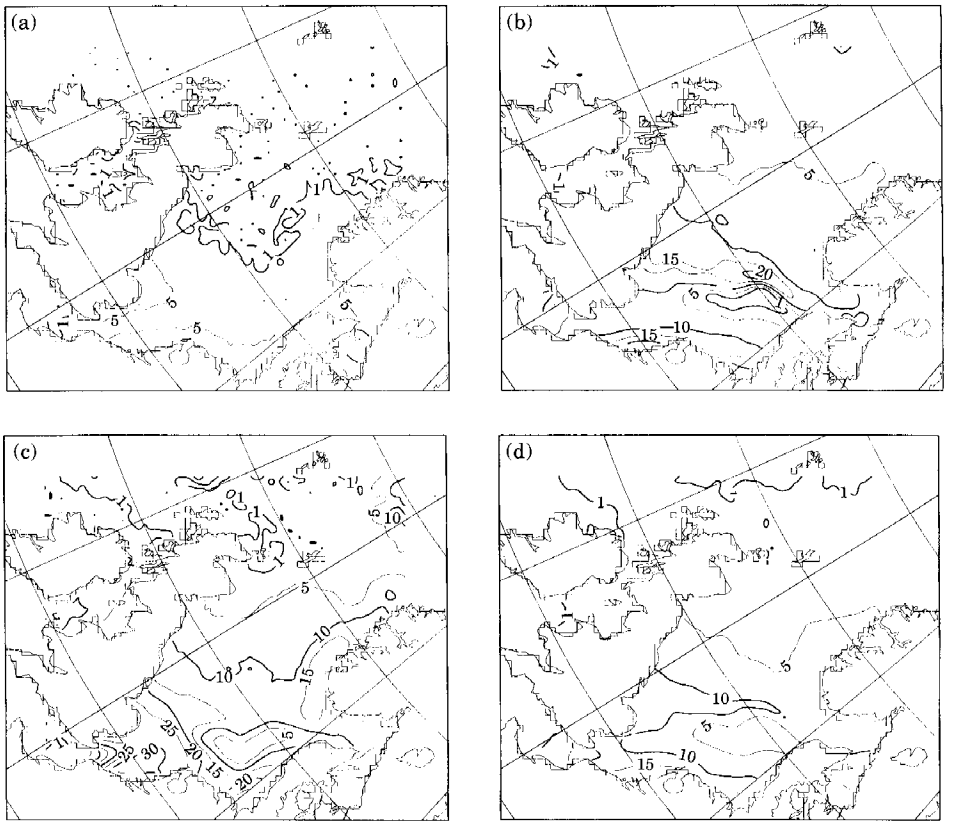

Figure 12. Reduction (in percentage) of flagellate production (g C m^{-2}) (a) during April (b) during June, (c) during August and (d) per annum with a 50% reduced anthropogenic load of nutrients to the model domain.

An additional estimate of the transport of inorganic nitrogen to Skagerrak (Figure 11) gives a reduction of *c.* 20% per annum when the anthropogenic loads of nutrients to the model domain are reduced, but almost all this reduction occurs during the second half of the model run, when the initial field becomes less important.

One should note that these results are the reductions during the first year. Since the initial fields were identical, the possible integrated effect of the reduction may increase through successive years, but in this aspect the longer term changes to the sediments (which are not included in the model) may be of great importance.

To get the best picture of the importance of eutrophication concerning the total food production it would be necessary to use an initial field without any anthropogenic nutrients. Such a field, together with no anthropogenic loads of nutrients to the model domain, would give a good approximation of the changes in the primary production that have occurred in the North Sea.

Another aspect of the total production is the recycling of nutrients. The paper of Howarth *et al.* (1993) shows, from an analysis of the winter nutrient budget, that recycling of nutrients in the water column is a major supplier. Our model agrees with this observation, in fact it seems that in some areas as much as 40% of the total production has its origin in recycled nutrients.

Clearly, the present lack of sedimentation and resuspension processes is probably the greatest weakness of the model system. In the shallower parts of the North Sea it is fair to assume that on an annual time-scale the sedimentation and resuspension of material are about the same. However, on seasonal and shorter time-scales, this is not the case. During strong winds, resuspension of nutrients (and other material) can cause sudden increased primary production (during the productive season), but at the same time reduced light due to increased turbidity will tend to reduce the production. During spring and summer with normally weak winds and strong production the sedimentation will in general be much stronger than the resuspension. With respect to nitrogen, this is in some areas partly compensated by denitrification (Aure & Dahl, 1994). During winter the resuspension is largely due to generally strong winds, and sedimentation of new organic material is low due to low production. Related to a possible strong reduction of anthropogenic nutrient inputs, in several regions there will probably be an unbalance in nutrient concentration at the water-bottom sediment interface with an adjustment scale of several years. In this process the sedimentation/resuspension process is probably important.

Conclusions

For the first time a 3-D baroclinic hydrodynamical model has been coupled to a chemical–biological model to study the primary production, transport and the possible effects of reduced input of anthropogenic nutrients throughout the North Sea.

Despite the very simple approach, the general quantitative and qualitative knowledge of the total yearly production, horizontal distribution and seasonal time evolution seems to be well simulated. The intercomparison with some salinity profiles also indicates that the model handles the large-scale circulation and vertical mixing fairly well.

Revealing the highly pulsating Jutland coastal water towards Skagerrak clearly shows the need for such models to be able to calculate realistic means of transported matter from one area to another.

The potential of using models to study the effects of, for example, reduced deposition of nutrients to the North Sea, makes them an important tool in political and environmental planning.

Acknowledgements

We thank Eivind Martinsen and co-workers at DNMI for providing an operational version of the physical module, including atmospheric and tidal forcing, and for providing the physical climatological fields adapted to our model region. Thanks also to the Norwegian Fisheries Science Foundation and the Norwegian State Pollution Control for providing financial support for this work.

References

Aksnes, D. L., Ulvestad, K. B., Baliño, B., Berntsen, J., Egge J. & Svendsen, E. 1995 Ecological modelling in coastal waters: Towards predictive physical-chemical–biological simulation models. *Ophelia* **41**, 5–36.

Aksnes, D. L. & Egge, J. K. 1991 A theoretical model for nutrient uptake in phytoplankton. *Marine Ecology Progress Series* **70**, 65–72.

Aksnes, D. L. & Lie, U. 1990 A coupled physical–biological pelagic model of a shallow Sill Fjord. *Estuarine, Coastal and Shelf Science* **31,** 459–486.

Aksnes, D. L., Aure, J., Furnes, G. K., Skjoldal, H. R. & Sætre, R. 1989 Analysis of the *Chrysochromulina Polyepis* bloom in the Skagerrak. May 1988. Environmental conditions and possible causes. *Bergen Scientific Centre, Technical Report* No. 1.

Anon. 1983 Flushing times of the North Sea. No. 123. *ICES, Technical Report.*

Anon. 1992 Guidance Document for the NSTF modelling workshop. 6–8 May 1992. The Hague.

Anon. 1993*a* Quality status report of the North Sea 1993. Report on subregion 1.

Anon. 1993*b* Quality status report of the North Sea 1993. Report on subregion 4.

Anon. 1993*c* Quality status report of the North Sea 1993. Report on subregion 5.

Anon. 1993*d* Quality status report of the North Sea 1993. Report on subregion 6.

Anon. 1993*e* Quality status report of the North Sea 1993. Report on subregion 7a.

Aure, J. & Dahl, E. 1994 Oxygen, nutrients, carbon and water exchange in the Skagerrak basin. *Continental Shelf Research* **14,** 965–977.

Blumberg, A. F. 1977 Numerical tidal model of Chesapeake Bay. *Journal of Hydraulics Division. ASCE* **103,** 1–10.

Blumberg, A. F. & Mellor, G. L. 1983 Diagnostic and prognostic numerical circulation studies of the South Atlantic Bight. *Journal of Geophysical Research* **88,** 4579–4592.

Blumberg, A. F. & Mellor, G. L. 1987 A description of a three-dimensional coastal ocean circulation model. In *Three-dimensional Coastal Ocean Models*, Vol 4 (Heaps, N., ed.). American Geophysical Union.

Cox, M. D. & Bryan, K. 1984 A numerical model of the ventilated thermocline. *Journal of Physical Oceanography* **14** 674–687.

Damm, P. 1989 Klimatologischer Atlas des Salzgehaltes, der Temperature und der Dichte in der Nord-see, 1968–1985. *Institute of Oceanography, University of Hamburg, Technical Report* No. 6-89.

Dundas, I., Johannessen, O. M., Berge, G. & Heimdal, B. 1989 Toxic algal bloom in scandinavian waters, May–June 1988. *Oceanography* **2.**

Egenberg, B. 1993 The relationship between hydrographical variability in coastal water and meteorological and hydrological parameters. M.Phil. Thesis, Geophysical Institute, University of Bergen, Norway (in Norwegian).

Eide, L. I., Reistad, M. & Guddal, J. 1985 Database av beregnede vind og bølgeparametre for Nordsjøen, Norskehavet og Barentshavet. *DNMI Report.*

Eppley, R. W. 1972 Temperature and phytoplankton growth in the sea. *Fishery Bulletin,* **70,** 1063–1085.

Gieskes, W. W. C. & Kraay, K. W. 1975 The phytoplankton spring bloom in Dutch coastal waters of the North Sea. *Netherlands Journal of Sea Research* **9,** 166–196.

Holligan, P. M. 1989 Primary production in the shelf seas in north-west Europe. *Advances in Botanical Research* **16,** 194–252.

Howarth, M. J., Dyer, K. R., Joint, I. R., Hydes, D. J., Purdie, D. A., Edmunds, H., Jones, J. E., Lowry, R. K., Moffat, T. J., Pomroy, A. J. & Proctor, R. 1993 Seasonal cycles and their spatial variability. *Philosophical Transactions of the Royal Society, Series A* **343,** 383–403.

Joint, I. & Pomroy, A. 1992 Phytoplankton biomass and production in the North Sea Results from the NERC North Sea project Aug 88–Oct 89. ICES. 8th meeting of the NSTF, Mont Saint-Mitchell, 19–22 May 1992.

Lancelot, C., Billen, G. & Rousseau, V. 1989 Joint EEC project on the dynamics of Phaeocystis blooms in nutrient enriched coastal zones. *University of Brussels, First Annual Progress Report.*

Maestrini, S. E. & Graneli, E. 1991. Environmental Conditions and Ecophysiological mechanisms which led to the 1988 *Chrysochromulina polylepis* bloom: an hypothesis. *Oceanologica Acta* **14,** 397–413.

Martinsen, E. A. & Engedahl, H. 1987 Implementation and testing of a lateral boundary scheme as an open boundary condition in a barotropic ocean model. *Coastal Engineering* **11,**603–627.

Martinsen, E. A., Slørdal, L. H. & Engedahl, H. 1990 MetOcean MOdeling Project (MOMOP), Phase 2, Data report: Joint presentation of the test cases. *The Norwegian Meteorological Institute, Technical Report No. 87.*

Martinsen, E. A., Engedahl, H., Ottersen, G., Ådlandsvik, B., Loeng, H. & Balino, B. 1992 MetOcean MOdeling Project. Climatological and hydrographical data for hindcast of ocean currents. *The Norwegian Meteorological Institute, Technical Report* No. 100.

Mellor, G. L. 1993 *User's Guide for a 3-dimensional, Primitive Equation, Numerical Ocean Model.*

Mellor, G. L. & Yamada, T. 1982 Development of a turbulence closure model for geophysical fluid problem. *Reviews of Geophysics and Space Physics* **20,** 851–875.

Mesinger, F. & Arakawa, A. 1976 Numerical methods used in atmospheric models. *GARP Publication Series, Technical Report* No. 17.

Oey, L.-Y. & Chen, P. 1991 A model simulation of circulation in the north-east Atlantic shelves and seas. *Stevens Institute of Technology Ocean Modeling Group, Contribution No. 6.*

Ottersen, G. 1991 MODgrid, a model oriented data grider. *Havforskningsinstituttet, Technical Report* No. 6/1991.

Rydberg, L. 1993. On the Skagerrak circulation and the supply of water from the southern North Sea to the Skagerrak. *Department of Oceanography, University of Gothenburg, Technical Report* No. 53,

Sathyendranath, S. & Platt, T. 1990 The light field in the ocean: its modification and exploitation by the Pelagi Biota. In *Light and Life in the Sea* (Herring, P. J., ed.). Cambridge University Press, Cambridge, pp. 333–344.

Skartveit, A. & Olseth, J. A. 1986 Modelling slope irradiance at high latitudes. *Solar Energy* **36,** 333–344.

Skartveit, A. & Olseth, J. A. 1987 A model for the diffuse fraction of hourly global radiation. *Solar Energy,* **37,** 271–274.

Skjoldal, H. R. 1993. Eutrophication and algal growth in the North Sea. In *Symposium Mediterranean Seas 200* (Della Croce, N. F. R., ed.). Universita di Genova, pp. 445–478.

Skjoldal, H. R. & Dundas, I. 1989. The *Chrysochromulina polylepis* bloom in the Skagerrak and the Kattegat in May–June 1988: environmental conditions, possible causes and effects. Report of the ICES workshop on the Ch.p. bloom in the Skagerrak and Kattegat. Bergen 28/2-2/3. 1989.

Skogen, M. D. 1993. A user's guide to NORWECOM, the NORWegian ECOlogical Model system. *Institute of Marine Research, Division of Marine Environment, Technical Report* No. 6, Bergen, Norway.

Slørdal, L. H., Martinsen, E. A. & Engedahl, H. 1991 MetOcean MOdeling Project (MOMOP), phase 2, final report: sensitivity tests and pre-operational simulations. *The Norwegian Meteorological Institute, Technical Report* No. 88.

Smagorinsky, J. 1963 General circulation experiments with the primitive equations, I. The basic experiment. *Monthly Weather Reviews* **91,** 99–164.

Stigebrandt. A. 1980. Barotropic and baroclinic response of a semi-enclosed basin to barotropic forcing of the sea. In *Proceeding of the NATO Conference on Fjord Oceanography* (Freeland, H. J., Farmer, D. M. & Levings, C. D., eds). Plenum Press, New York.

de Vries, I. (ed.) 1992 Report of the NSTF modelling workshop. *Tidal Waters Division, The Hague, Report* No. DGW-92.045.

Appendix A

The biological model

Incident irradiation

The incident irradiation is modelled using a formulation of Skartveit and Olseth (1986, 1987). The irradiance is split into a diffuse and a direct component

$$H_x(h,n)=I_0(n)\ Tr_{0x}(n)\ F_x(h) \tag{A1}$$

Here, $H_x(h,n)$ is either direct (x=dir) or diffuse (x=dif) irradiance at the surface; $I_0(n)$ is the solar irradiance at normal incidence just outside the atmosphere; and $Tr_{0x}(n)$ the transmittance at overhead zenith sun given by:

$$\mathrm{Tr}_{0x}(n)=a_x\left(1+b_x\cos\frac{n-c_x}{365}2\pi\right) \tag{A2}$$

$F_x(h)$, the solar elevation function, is estimated in every internal time step, and is given by:

$$F_x(h)=d_x+e_x\sin h-f_x(\sin h)^{1/2} \tag{A3}$$

where h is the solar elevation and n the day number.

This model gives a climatological light formulation as function of the area dependent constants $a_x \ldots f_x$. An interpolation technique (Aksnes *et al.*, 1995) for these constants has been developed to include data for total daily irradiance. Light measurements from Texel (Anon., 1992) have been used and assumed valid for the

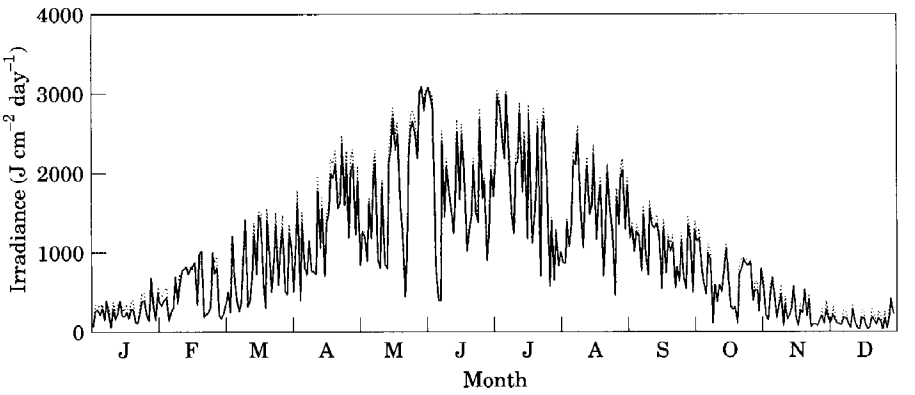

Figure 13. Modelled integrated daily global irradiance (· · · ·) *vs.* real measurements (————) at Texel (54°N).

whole model area. In Figure 13, modelled and measured total daily irradiance during 1985 are compared. The formulas are valid when the solar elevation is above 5 °; nevertheless, they have been used for all solar elevations.

Light in the water column

The diffuse light is calculated from

$$I_{\mathrm{dif}}(x,y,z,t) = PAR \cdot R_{\mathrm{dif}}(x,y,t) e^{\frac{-\kappa(x,y,z,t)}{\mu}} \tag{A4}$$

where $R_{\mathrm{dif}}(x,y,t) = H_{\mathrm{dif}}\ (h,n)$, the diffuse component of the surface irradiance, and PAR is a constant which converts incident diffuse irradiation to photosynthetic available radiance, μ is the mean cosine of the diffuse light (Sathyendranath & Platt, 1990), and κ is the attenuation coefficient:

$$\kappa = b_2 z + \frac{v}{N2Chla} \int_0^z (DIA(x,y,z,t) + FLA(x,y,z,t))dz \tag{A5}$$

Here, v is the chlorophyll a light extinction coefficient, $N2Chla$ the fraction of nitrate and chlorophyll a in a cell, and b_2 extinction due to water and other substances.

A similar formulation to equation (A4) is given for the direct light, $I_{\mathrm{dir}}(x,y,z,t)$, by substituting R_{dif} with R_{dir} and μ with cos φ, where φ is the zenith angle of the direct light in the water column.

Primary production

The concentration of chlorophyll in the system is affected by the production of the algae, their death and by respiration. Since zooplankton is not included in the model, the grazing is (very roughly) included in the constant death rate of 0·1 day^{-1}.

The relationships between phytoplankton production and light intensity, and between phytoplankton production and nutrient uptake are represented by an affinity formulation (Aksnes *et al.*, 1995). The combined effects of nutrient and light limitation are multiplicative and given by:

$$\mu_{dia}(x,y,z,t) = \mu_{max} V_1 N_{lim} Dia, \quad N_{lim} = \min_{2 \le i \le 4} V_i \tag{A6}$$

where

$$V_i = \frac{S_i}{S_i + \frac{\mu_{max}(T)}{\alpha_i}}, \quad i = 1, \ldots, 4 \tag{A7}$$

is a modified Michaelis–Menten limitation for substance S_i. In the equations, $i=1$ corresponds to irradiance, $i=2$ to nitrate, $i=3$ to phosphate and $i=4$ to silicate. In this formulation the use of constant half-saturation parameters, K_s, have been avoided. According to Aksnes and Egge (1991), K_s values are made temperature dependent through the affinity parameter, a_i, defined as:

$$\alpha_i = \frac{\mu_{max}(T_0)}{K_{S_i}} \tag{A8}$$

where K_{S_i} is the conventional half-saturation constant at temperature T_0; μ_{max} is the specific growth rate of the population under optimum light and nutrient conditions and made temperature dependent as suggested (Eppley, 1972). The relation

$$\mu_{max}(x,y,z,t) = a_1 \, e^{a_2 T(x,y,z,t)} \tag{A9}$$

has been chosen.

The metabolic losses are assumed to be related to the temperature according to the equation.

$$R_{dia} = a_5 \, Dia \, e^{a_6 T(x,y,z,t)} \tag{A10}$$

and the death (in the whole water column) is assumed to be at a constant rate as long as the concentration of the algae somewhere in the column is above an minimum level. Below this level the death rate is zero, in order to prevent the algae in the model becoming extinct because of light limitation during the winter.

All of these expressions refer to diatoms. Analogous formulations are used for the flagellates, except that silicate is not rate-limiting for them. The biological parameter values were chosen according to independent validation against mesocosmos experiments (Aksnes *et al.*, 1995).

Appendix B

Parameter values

Parameter	Explanation	Value
PAR	Photosynthetic active irradiance	40%
μ	Mean cosine of diffuse light zenith angle	0·83
ν	Chl *a* light extinction coefficient	1·38E-2 (m mg Chl a^{-1})
N2Chla	Cellular fraction of nitrate and Chl *a*	11·0 (mg N mg Chl a^{-1})
$a(1)$	Diatom production maximum at 0 °C	1·53E-5 (s^{-1})
$a(2)$	Diatom temperature dependent P_{max}	0·063 ($°C^{-1}$)
$a(3)$	Flagellate production maximum at 0 °C	1·02E-5 (s^{-1})
$a(4)$	Flagellate temperature dependent P_{max}	0·063 ($°C^{-1}$)
$a(5)$	Metabolic loss rate at 0 °C	805E-7 (s^{-1})
$a(6)$	Metabolic loss rate temperature dependence	0·07 ($°C^{-1}$)
$c(1)$	Intercellular P/N relationships	0·138 (mg P mg N^{-1})
$c(2)$	Intercellular Si/N relationship	1·75 (mg Si mg N^{-1})
$c(3)$	Death rate (0·1)	1·6E-6 (s^{-1})
$c(4)$	Rate of decomposition detritus (0·013)	1·52E-7 (s^{-1})
a_{d1}	Growth affinity for irradiance (diatoms)	3·6E-7 (m^2 μEinstein $^{-1}$)
a_{d2}	Growth affinity for nitrate (diatoms)	1·7E-5 (s^{-1} μM^{-1})
a_{d3}	Growth affinity for phosphate (diatoms)	2·7E-4 (s^{-1} μM^{-1})
a_{d4}	Growth affinity for silicate (diatoms)	2·5E-5 (s^{-1} μM^{-1})
a_{d1}	Growth affinity for irradiance (flagellates)	1·1E-7 (m^2 μEinstein^{-1})
a_{d2}	Growth affinity for nitrate (flagellates)	1·5E-5 (s^{-1} μM^{-1})
a_{d3}	Growth affinity for phosphate (flagellates)	2·5E-4 (s^{-1} μM^{-1})
s_1	Sinking rate diatoms (SIL dependent)	3E-6 $\leq s_1 \leq$ 3E-5 (m s^{-1})
s_2	Sinking rate flagellates	2·9E-6 (m s^{-1})
s_3	Sinking rate detritus	3·5E-5 (m s^{-1})